

# Biogenic synthesis and spectroscopic characterization of silver nanoparticles using leaf extract of *Indoneesiella echioides*: in vitro assessment on antioxidant, antimicrobial and cytotoxicity potential

Gunaseelan Kuppurangan<sup>1</sup> · Balaji Karuppasamy<sup>1</sup> · Kanipandian Nagarajan<sup>1</sup> · Rajkumar Krishnasamy Sekar<sup>1</sup> · Nilmini Viswaprakash<sup>3</sup> · Thirumurugan Ramasamy<sup>1,2</sup>

Received: 8 July 2015 / Accepted: 29 November 2015 / Published online: 31 December 2015  
© The Author(s) 2015. This article is published with open access at Springerlink.com

**Abstract** Natural synthesis of metal nanoparticles is gaining more attention in recent years. This article demonstrates the phytochemical synthesis of silver nanoparticles (AgNPs) by using *Indoneesiella echioides* (L) leaf extract as a reducing and stabilizing agent. Biosynthesis of AgNPs was monitored by UV–visible spectroscopy which revealed intense surface plasmon resonance bands at 420 nm. Fourier transform infrared spectroscopy (FTIR) and X-ray diffraction were employed to identify various functional groups and crystalline nature of AgNPs. High-resolution transmission electron microscopy studies demonstrated that synthesized particles were spherical with average size of ~29 nm. In vitro antioxidant effects were analyzed by 2,2'-Azino-bis-(3-ethylbenzothiazoline-6-sulfonic acid) diammonium salt (ABTS) and 2,2-diphenyl-1-picrylhydrazyl (DPPH), which exhibited 69 and 71 % of scavenging activity, respectively. The antimicrobial activity of green AgNPs displayed better zone of inhibition against selected human pathogens. The present study also investigated the toxicity effect of biogenic AgNPs against human lung adenocarcinoma cancer cells (A549) and normal human epithelial cells (HBL-100) in vitro, and the inhibitory concentrations (IC<sub>50</sub>) were found

to be 30 and 60 µg/mL, respectively. Herein, we propose a previously unexplored medicinal plant for the biological synthesis of AgNPs with potent biomedical applications.

**Keywords** *Indoneesiella echioides* · Silver nanoparticles · X-ray diffraction · Transmission electron microscope · Cytotoxicity

## Introduction

In recent times, stupendous efforts have been taken for the development of efficient methodology for the synthesis of metal nanoparticles with unique physicochemical and optoelectronic properties and their important applications in optics, electronics, biomedicine, magnetic, mechanics, catalysis, energy science, and so on (Dua and Jiang 2007). The synthesis of monodispersed nanoparticles with different sizes and shapes has been a great challenge in nanotechnology. Although various physical and chemical methods are extensively used to produce monodispersed nanoparticles, the stability and the use of toxic chemicals are the subjects of paramount concern (Rao and Cheetham 2001). The secrets discovered from nature have led to the development of biomimetic approaches to the growth of advanced nanomaterials (Singaravelu et al. 2007).

Green-assisted synthesis of nanoparticles using plant materials are effortless, capable and eco-friendly in comparison with chemical-mediated or microbe-mediated synthesis (Anamika et al. 2012). In combination with metallic nanoparticles such as copper, zinc and silver are most promising because of their biomedical properties. However, the mechanism and mode of action are still a matter of debate, due to their superior antimicrobial properties against bacteria, viruses and fungi comparing with

✉ Thirumurugan Ramasamy  
ramthiru72@gmail.com

<sup>1</sup> Laboratory of Aquabiotics/Nanoscience, Department of Animal Science, School of Life Sciences, Bharathidasan University, Tiruchirappalli, Tamilnadu 620 024, India

<sup>2</sup> School of Fisheries, Aquaculture and Aquatic Sciences, Auburn University, Auburn, AL 36849-5419, USA

<sup>3</sup> Department of Biomedical Sciences, College of Veterinary Medicine, Nursing and Allied Health, Tuskegee University, Tuskegee, AL 36088, USA

standard antibiotics (Rai et al. 2009; Weir et al. 2008). Green-prepared silver nanoparticles (SNPs) have the physical properties of a larger specific surface area, smaller in size and high dispersion (Sharma et al. 2009). We have selected *Indoneesiella echioides*, an herbal plant widely scattered in the dry places of stiffer India and Sri Lanka (Gamble 1956). In Indian traditional medicine, the leaf extract of *I. echioides* was used as a remedy for fever (Kirtikar and Basu 1975) and also the plant from genus *Andrographis* is used to treat goiter, liver diseases (Nadkarni and Nadkarni 1976), fertility disorders, bacterial (Qadrie et al. 2009), malarial and fungal diseases. These phytochemically synthesized SNPs have a potential effect such as good nanostructure (Huh and Kwon 2011) and antibacterial (Savithamma et al. 2011), antioxidant (Swamy et al. 2014) and anticancer activity (Vasanth et al. 2014).

This present investigation deals with the biosynthesis of silver nanoparticles using *I. echioides* leaf extract as a reducing and stabilizing agent; antioxidant activity of biosynthesized AgNPs was evaluated for ABT and DPPH assays and also antibacterial activity against gram-positive (*Rhodococcus rhodochrous*), gram-negative (*Aeromonas hydrophila*, *Staphylococcus aureus*, *Pseudomonas aeruginosa*) bacterial pathogens and fungal pathogen (*Candida albicans*). Furthermore, the anticancer activity of synthesized silver nanoparticles was examined in human lung adenocarcinoma cancer cell line (A549) and normal human epithelial cells (HBL-100).

## Materials and methods

### Preparation of plant extract

The healthy, matured and disease-free leaves of *I. echioides* were collected (Kolli Hills, Namakkal District, Tamil Nadu, India) and rinsed thoroughly in deionized water. Then, the cleaned leaves were sterilized using 0.02 % mercuric chloride. The sterilized leaves were then dried and finely powdered. The extract was prepared by mixing 2.5 g of the powdered leaf in 100 mL of deionized water, and this mixture was boiled at 80 °C for 5 min before decanting.

### Synthesis of Ag nanoparticles

For the synthesis of silver nanoparticles, 5 mL of *I. echioides* leaf extract was added dropwise into 45 mL of 1 mM silver nitrate (HiMedia) with constant stirring. As soon as *I. echioides* extract was mixed in an aqueous solution of silver ions, the reaction mixture turned from whitish to yellowish brown color. Finally, the samples were

centrifuged at 6000 rpm for 20 min, and pellet was lyophilized, and nanoparticles were stored at 4 °C.

## Characterization of silver nanoparticles

### UV–Vis spectra and FTIR analysis

The bioreduction of Ag<sup>+</sup> ions in solution was monitored using UV–visible spectroscopy (Synergy HT Multi-mode Microplate Reader, Bio-Tek Instruments, Inc., Winooski, VT, USA). Further, Fourier transform infrared spectroscopy (FTIR) measurements were taken using JASCO (FT/IR-6200) spectrophotometer to identify the functional groups in the dried form of SNPs and the plant leaf powder.

**XRD measurement** After bioreduction, the residual solutions consisting of hydrosols and biomass were dried at 60 °C, and the dried mixture was collected for the determination of the formation of Ag by an X'Pert Pro X-ray diffractometer (PANalytical BV, The Netherlands) operated at a voltage of 40 kV and a current of 30 mA with Cu K $\alpha$  radiation. The  $2\theta$  values were calculated by using the Debye–Scherrer's formula,  $D = 0.9 \lambda / \beta \cos \theta$ , where D is the mean diameter of the nanoparticles,  $\lambda$  is the wavelength of X-ray radiation source, and  $\beta$  is the angular FWHM of the XRD peak at the diffraction angle  $\theta$ .

**High-resolution transmission electron microscopy (HR-TEM) analysis** Surface morphology and size of silver nanoparticles were determined by HR-TEM. A sample of the aqueous suspension of silver nanoparticles was prepared by placing a drop of the suspension on carbon-coated copper grids and allowing water to evaporate. TEM observations were performed on electron microscope (TechnaiG2 analyzer). Size distribution of the resulting nanoparticles was estimated on the basis of TEM micrographs. High-resolution TEM images were obtained, and crystalline structure was confirmed with the help of SAED pattern.

### In vitro antioxidant assay

#### ABTS scavenging assay

2,2'-Azino-bis (3-ethylbenzothiazoline-6-sulfonic acid) diammonium salt (ABTS) scavenging activity was determined by modified method described by Rameshkumar and Sivasudha (2012). The working solution was prepared by mixing two stock solutions of 7 mM ABTS solution and 2.4 mM potassium persulfate solution in equal amounts and allowed to react for 12 h at room temperature in the dark condition. One milliliter of the resulting solutions was allowed to react with 1 mL of the aqueous nanoparticles in

different concentration ranging from 10 to 50  $\mu\text{g/mL}$ , and the reaction mixture was vortexed, and absorbance was measured at 734 nm after 6 min interval. Similar procedures were carried out for the butylated hydroxytoluene (BHT) standard at various concentrations. The percentage of inhibition capacity of ABTS by the silver nanoparticles was calculated from the following equation;

$$\text{ABTS scavenging activity(\%)} = \frac{(A_o - A_t)}{A_o} \times 100 \quad (1)$$

where  $A_o$  control absorbance and  $A_t$  sample absorbance.

#### DPPH scavenging assay

2,2-Diphenyl-1-picrylhydrazyl (DPPH) assay was carried out using modified method described by Rameshkumar and Sivasudha (2012). One milliliter of 0.135 mM DPPH prepared in methanolic was mixed with 1 mL of aqueous nanoparticles with various concentrations ranging from 10 to 50  $\mu\text{g/mL}$ . The reaction mixture was vortexed thoroughly and left in dark at room temperature for 30 min. The percentage of inhibition capacity of DPPH by the silver nanoparticles was calculated from Eq. 1.

#### Agar diffusion assay

Microbial cultures were grown overnight in nutrient broth medium and centrifuged at 5000 rpm for 2 min. Then, the pellet was washed with  $1 \times$  PBS and resuspended in fresh nutrient broth medium and allowed to grow for 6 h. The 100  $\mu\text{L}$  of the suspended cultures (gram-positive *Rhodococcus rhodochrous* (MTCC 265), gram-negative bacterial pathogens *Aeromonas hydrophila* (MTCC 1739), *Staphylococcus aureus* (MTCC 2940), *Pseudomonas aeruginosa* (MTCC 2453) and fungal pathogen *Candida albicans* (MTCC 227)) was spread uniformly on nutrient agar plates, and the plates were incubated at 37  $^\circ\text{C}$  for 30 min. The AgNPs at different concentrations (100, 150 and 200  $\mu\text{g/mL}$ ) were loaded into the wells. The zone of inhibition was determined by measuring the diameter (mm) of bacterial clearance after 24 h.

#### Assessment of in vitro cytotoxicity

The cancer cell line A549 and normal human epithelial cells (HBL-100) were purchased from the National Center for Cell Sciences (NCCS, Pune, India). The cells were maintained in Dulbecco's modified eagles medium (DMEM) and McCoy's 5a medium, respectively, in supplement with non-essential amino acids. The cells were maintained at 37  $^\circ\text{C}$  with 5 %  $\text{CO}_2$  in a humidified  $\text{CO}_2$  incubator. The cells were seeded ( $1 \times 10^4$  cells/well) in a 96-well plate and incubated for 48 h into 75 % confluence.

The medium was replaced with fresh medium containing serially diluted AgNPs, and the cells were further incubated for 48 h. The culture medium was removed, and 100  $\mu\text{L}$  of the MTT [3-(4,5-dimethylthiazol-2-yl)-3,5-diphenyl tetrazolium bromide] (HiMedia) solution was added to each well and incubated at 37  $^\circ\text{C}$  for 4 h. Purple color formazan crystals were observed, and these crystals were dissolved with 100  $\mu\text{L}$  of dimethyl sulfoxide (DMSO) and read at 620 nm in a multi-well ELISA plate reader (Thermo, Multiskan, USA). Optical density (OD) value was subjected to sort out percentage of viability by using the following formula

$$\begin{aligned} \text{Percentage of viability} \\ = \frac{\text{Absorbance of experimental sample (AgNPs treated)}}{\text{Absorbance of experimental control (untreated cells)}} \times 100 \end{aligned} \quad (2)$$

#### Observation of cytomorphological alterations

The A549 and HBL-100 cells that were grown on cover slips ( $1 \times 10^5$  cells/cover slip) were incubated with biogenic AgNPs at the  $\text{IC}_{50}$  concentration and then fixed in methanol:acetic acid solution (3:1, v/v). The cover slips were gently mounted on glass slides for the morphometric analysis. The morphological changes in AgNPs-treated A549 and HBL-100 cells were analyzed using Nikon (Japan) bright field inverted light microscopy at 400  $\times$  magnification.

## Result and discussion

### Characterization of silver nanoparticles

Synthesized silver nanoparticles were initially identified by the color change in the reaction from yellow to brown color. Further confirmation was done by UV–visible

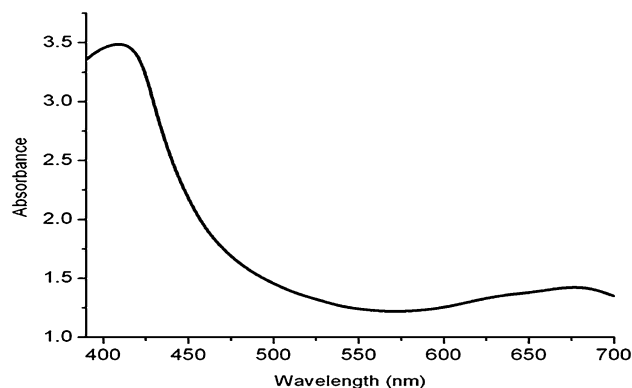
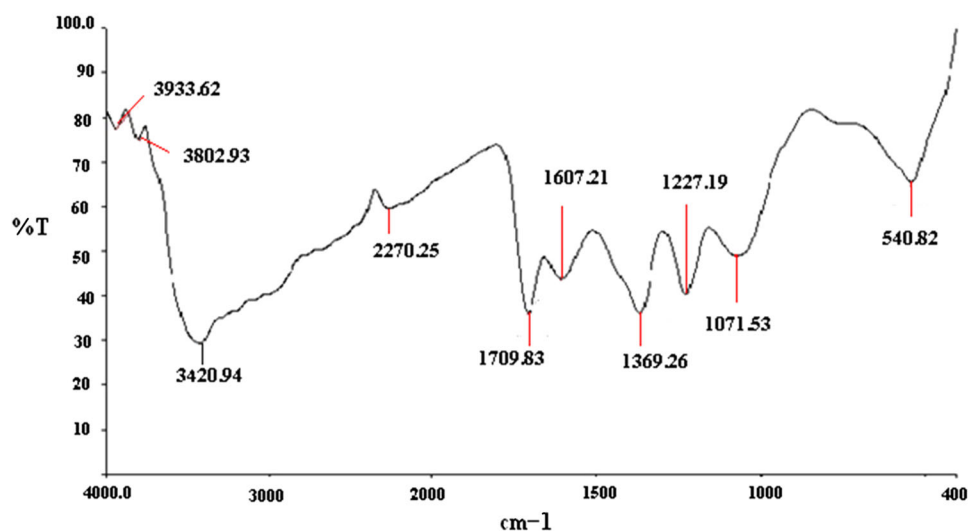


**Fig. 1** UV–visible spectroscopy of biosynthesized silver nanoparticles (AgNPs)

**Fig. 2** FTIR spectrum of AgNPs showed the presence of different functional groups



spectroscopy (Fig. 1). UV–visible spectroscopy has shown the absorption peak at 420 nm. An UV–visible spectrum is one of the important techniques to verify the formation of metal nanoparticles provided surface plasmon resonance exists for that metal. It is known from the spectra that the silver surface plasmon resonance band occurs between 410 and 420 nm (Maliszewska et al. 2009; Ashok et al. 2010; Kaviya et al. 2011; Kanipandian and Thirumurugan 2014).

The powdered form of prepared silver nanoparticles was used for FTIR analysis to identify the presence of functional groups which are responsible for reduction of AgNPs from plant leaf. The intensity peak values ranging from  $\sim 3420.94$ , 2270.25, 1709.83, 1160.21, 1369, 1227.19, 1071.53 and  $540.82 \text{ cm}^{-1}$  were identified. Figure 2 and Table 1 represent the FTIR spectra and corresponding functional groups of synthesized AgNPs from the *I. echinoides* plant leaf extract. The following functional groups were identified such as aromatic primary amine (C–N stretch), secondary amine N–H bend, organic nitrates, carbonate ions and aliphatic fluoro compounds C–F stretch. The IR bands at  $\sim 1709.83$  and  $1369 \text{ cm}^{-1}$  are characteristic of C–O and C–O stretching modes, respectively, of the carboxylic group (Kathiraven et al. 2015). The strong band at  $\sim 1037 \text{ cm}^{-1}$  arises from C–O–C and C–OH vibrations (Solomun et al. 2004; Ankamwar et al. 2005; Huang et al. 2007; Li et al. 2007; Kannan and Abraham John 2008). Earlier studies revealed that the absorbance bands at  $\sim 1109$  and  $1726 \text{ cm}^{-1}$  in curve were associated with the stretch vibration of –C–O and –C=C respectively (Zhu 2000). Hence, it is possible that proteins/enzymes play a vital role in reduction of metal ions by the oxidation of aldehydes to carboxylic acid. Amide II band is observed at  $\sim 1538 \text{ cm}^{-1}$ , and amide I band got merged in the broad envelope around  $\sim 1743 \text{ cm}^{-1}$  (Solomun et al. 2004).

**Table 1** FTIR analysis of phytosynthesized silver nanoparticles

| Wave frequency $\text{cm}^{-1}$ | Functional groups of AgNPs             |
|---------------------------------|--|
| 3420.94                         | Aromatic primary amine NH stretch      |
| 2270.25                         | Aliphatic cyanide/nitrate              |
| 1709.83                         | Carboxylic acid                        |
| 1160.21                         | Secondary amine, NH bend               |
| 1369.26                         | Nitrate ion                            |
| 1227.19                         | Aromatic phosphates (P–O–C stretch)    |
| 1071.53                         | Aliphatic fluoro compounds C–F stretch |
| 540.82                          | Aliphatic iodo compounds C–I stretch   |

### XRD analysis

The XRD analysis (Fig. 3) shows that the diffraction peaks at  $2\theta$  are  $38.10^\circ$ ,  $44.22^\circ$ ,  $64.52^\circ$  and  $77.36^\circ$  and can be assigned to the (1 1 1), (2 0 0), (2 2 0) and (3 1 1) planes of a face-centered cubic (fcc) structure of silver nanoparticles compared with JCPDS card no: 65-2871 (Yugandhar and Savithamma 2015). XRD patterns were analyzed to determine peak intensity, position and full width at half maximum (FWHM) data were used with the Debye–Scherrer’s formula to determine the crystallite size, and the estimated crystallite size was 19 nm. Further, the silver nanoparticles were crystalline nature, and the current XRD data were well correlated with the existing literature (Ashok et al. 2010; Shashi Prabha et al. 2010; Dwivedi and Gopal 2010).

### HR-TEM analysis and SAED pattern

HR-TEM was employed to analyze the morphology and size of biosynthesized AgNPs. TEM studies demonstrated

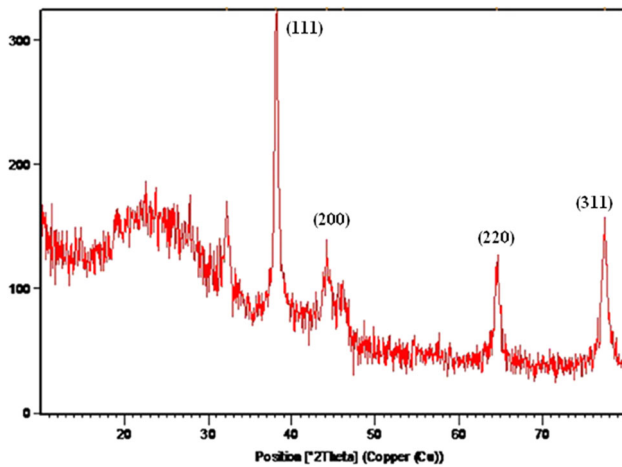


**Fig. 3** XRD image represents the crystalline nature of AgNPs

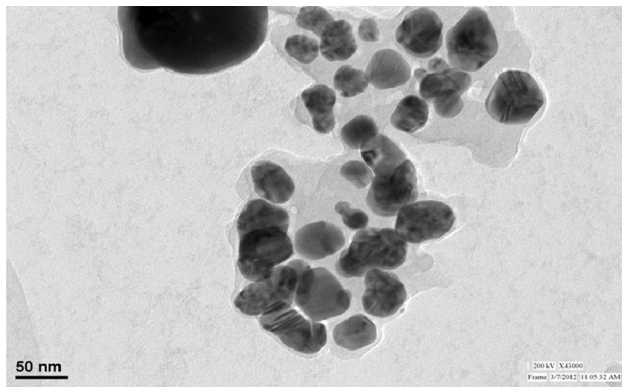


**Fig. 4** HR-TEM image depicts the spherical structure of phytosynthesized AgNPs

that synthesized particles were spherical with average size of  $\sim 29$  nm (Fig. 4). Figure 5 shows that the selected-area electron diffraction (SAED) pattern of green-synthesized AgNPs confirms the crystalline (fcc) nature of the silver nanoparticles (Rajkumar et al. 2015).

### In vitro antioxidant assay

Figure 6 displays the antioxidant image of the green-synthesized AgNPs. The ABTS assay was used to detect the antioxidant property of AgNPs depicted in Fig. 6a. The highest percentage of inhibition was found to be 71 % at 1000  $\mu\text{g}/\text{mL}$  concentration of AgNPs, and BHT (standard) exhibited 81 % of scavenging ability at the same concentration.

DPPH assay was used to determine the high antioxidant potential of AgNPs and is shown in Fig. 6 (b). The highest percentage of inhibition was found to be 69 %, and BHT (control) displayed 81 % at 1000  $\mu\text{g}/\text{mL}$ .

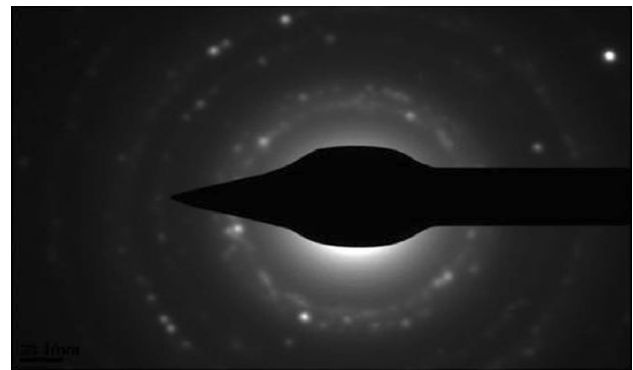


**Fig. 5** SAED pattern for AgNPs

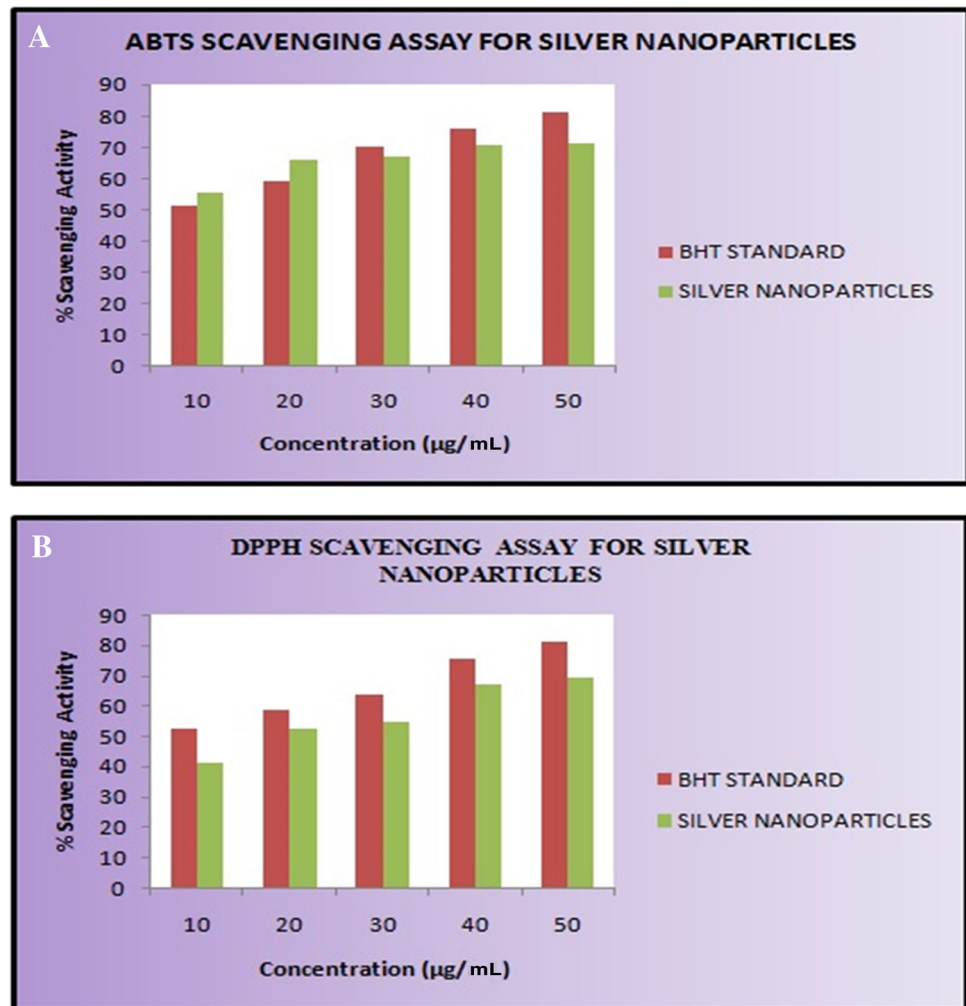
The involvement of active oxygen and free radicals in the pathogenesis of certain human diseases, including cancer, aging and atherosclerosis, is increasingly being recognized (Moskovitz et al. 2002). Active oxygen and free radicals, such as superoxide anion ( $\text{O}_2^-$ ), hydrogen peroxide ( $\text{H}_2\text{O}_2$ ) and hydroxyl radical ( $\text{OH}\cdot$ ), are constantly formed in the human body by normal metabolic action. Their action is opposed by a balanced system of antioxidant defenses, including antioxidant compounds and enzymes. Upsetting the radical balance causes oxidative stress, which can lead to cell injury and death (Halliwell and Gutteridge 1999). Therefore, much attention has been focused on the use of antioxidants, especially natural antioxidants, to inhibit or to protect against the damage of free radicals (Vendemiale et al. 1999). This investigation provides evidence for the uses of biosynthesized silver nanoparticles as natural antioxidant or potential radical scavenger against deleterious damages caused by the free radicals.

### Antimicrobial activity of silver nanoparticles

The well diffusion method was used to evaluate the antimicrobial activity of silver nanoparticles against the pathogens such as gram-positive bacteria *Rhodococcus rhodochrous* (MTCC 265), gram-negative bacterial pathogens *Aeromonas hydrophila* (MTCC 1739), *Staphylococcus aureus* (MTCC 2940), *Pseudomonas aeruginosa* (MTCC 2453) and fungal pathogen *Candida albicans* (MTCC 227). The zone of inhibition tests were conducted for three different concentrations (100, 150 and 200  $\mu\text{g}/\text{mL}$ ) of Ag nanoparticles. The potent antimicrobial nature of the silver nanoparticles was confirmed by the zone of inhibition around the wells. Figure 7 and Table 2 indicate the diameter of zone of inhibitions formed around the colonies of microorganisms.

Previous studies have revealed that ionic silver has the property to strongly interact with thiol groups of vital enzymes and inactivate the bacterial cells. Experimental

**Fig. 6** In vitro antioxidant potential of AgNPs using ABTS (a) and DPPH (b) scavenging assay



evidence has shown that DNA loses its replication ability once the bacteria have been treated with silver ions (Jose Ruben et al. 2005). Most importantly, silver attacks a broad range of targets in the microbes, so it is difficult for them to develop resistance against silver, because this would require developing a host of mutations to protect themselves (Sharvil et al. 2009). Our findings proved the capability of silver nanoparticles to inhibit the pathogens, and it suggests that AgNPs can be used for antimicrobial applications.

#### Anticancer efficacy of biogenic AgNPs

Silver nanoparticles are gaining more attention from research community and also from the biomedical industry for their potential biomedical applications. At the same time, only limited studies were conducted to evaluate the anticancer effects of biologically synthesized AgNPs,

against cancer cell lines. In this study, an in vitro cytotoxicity assay for AgNPs on A549 and HBL-100 cells was conducted using an MTT reduction assay (Fig. 8). After the treatment of cells with different concentrations (10–100 µg/mL) of AgNPs, the inhibitory percentage against proliferation of cells was determined. The cytotoxicity effect on A549 cell lines was increased with increased concentration of AgNPs. In the present study, dose-dependent cytotoxicity was observed in AgNPs-treated A549 cells, and fifty percentage of cancer cell death ( $IC_{50}$ ) was found to be at the silver nanoparticle concentration of 30 µg/mL. The HBL-100 cells failed to show cytotoxic effect at lower concentrations, and cytotoxicity increases with increasing concentration of AgNPs by 60 µg/mL. It is evident from these results that when compared to the cancer cells  $IC_{50}$  concentration (30 µg/mL), control/normal cells used for this study required double the volume (60 µg/mL), i.e., silver nanoparticles at a concentration of 30 µg/mL were non-toxic to control/

**Fig. 7** Antimicrobial activity of AgNPs synthesized from *Indoneesiella echioides*. Assayed plates show the zone of inhibition around the colonies of pathogenic microorganisms at various concentrations (100, 150 and 200  $\mu\text{g}/\text{mL}$ ) of silver nanoparticles

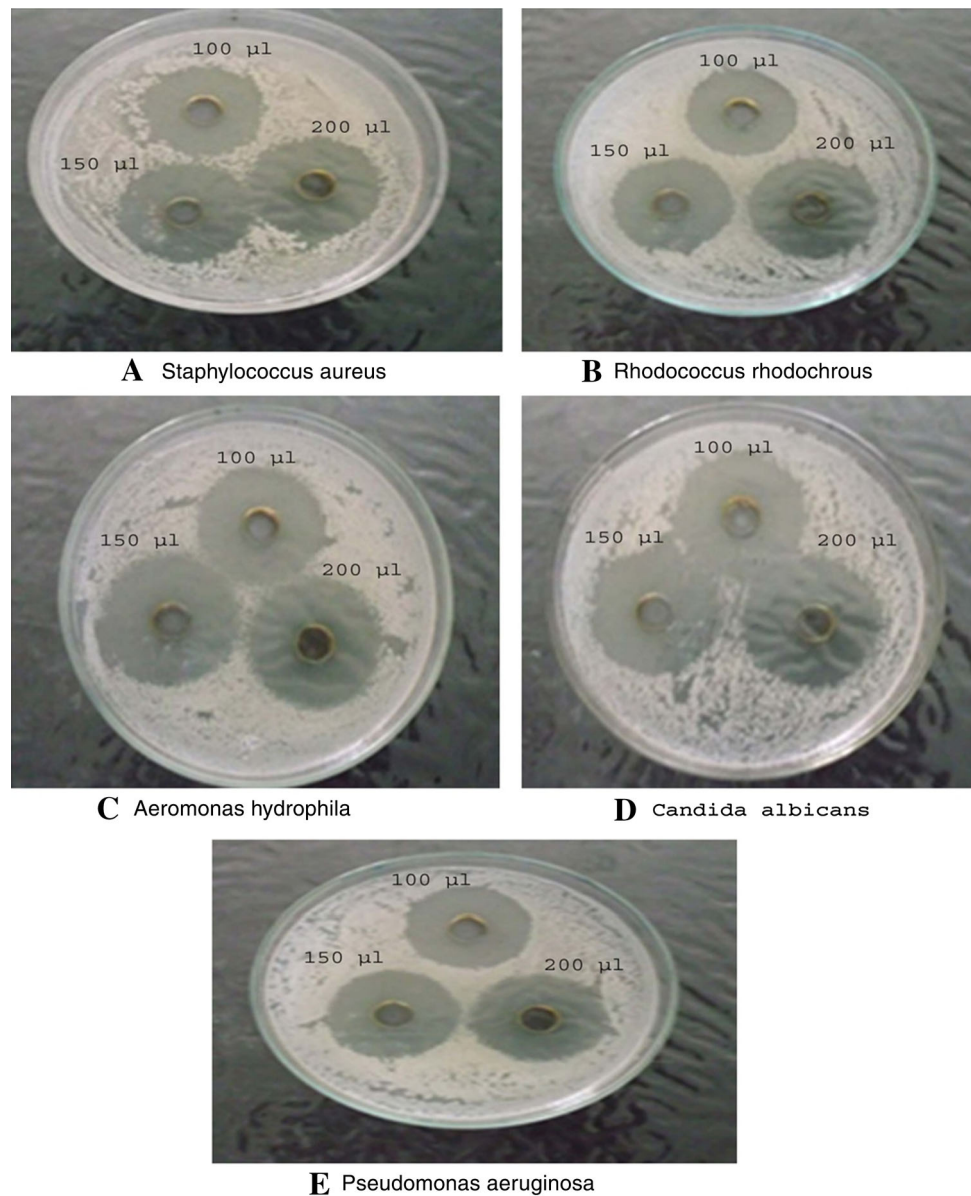


**Table 2** Zone of inhibition of silver nanoparticles against different microorganisms via agar well diffusion method

| S. no. | Microorganism                  | Zone of inhibition (mm)     |                             |                             |
|--------|--------------------------------|-----------------------------|-----------------------------|-----------------------------|
|        |                                | 100 $\mu\text{g}/\text{mL}$ | 150 $\mu\text{g}/\text{mL}$ | 200 $\mu\text{g}/\text{mL}$ |
| 1      | <i>Candida albicans</i>        | 32                          | 34                          | 35                          |
| 2      | <i>Aeromonas hydrophila</i>    | 31                          | 34                          | 36                          |
| 3      | <i>Staphylococcus aureus</i>   | 30                          | 32                          | 34                          |
| 4      | <i>Rhodococcus rhodochrous</i> | 30                          | 31                          | 32                          |
| 5      | <i>Pseudomonas aeruginosa</i>  | 28                          | 30                          | 31                          |

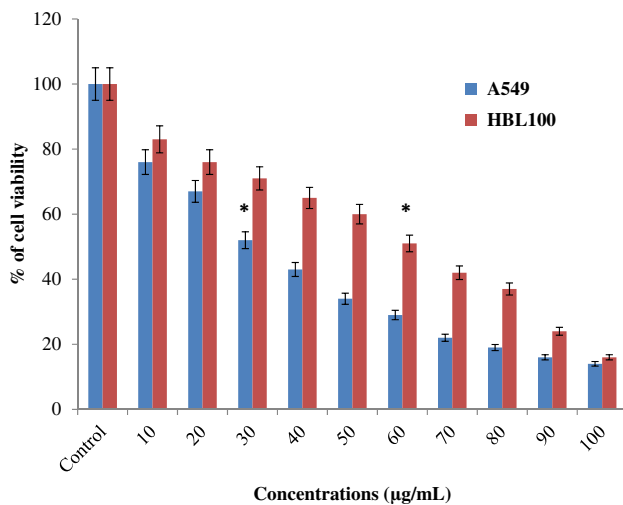


**Fig. 8** Cytotoxicity effect of green-synthesized AgNPs against A549 cancer and HBL-100 normal cell lines (*asterisk* significant  $IC_{50}$  concentrations)

normal cells. Our present findings provide the evidence for cytotoxic effect of biogenic AgNPs from extract of *I. echioides* against lung cancer A549 cell line compared with HBL-100 normal cell lines.

#### Morphological analysis of AgNPs-treated cells

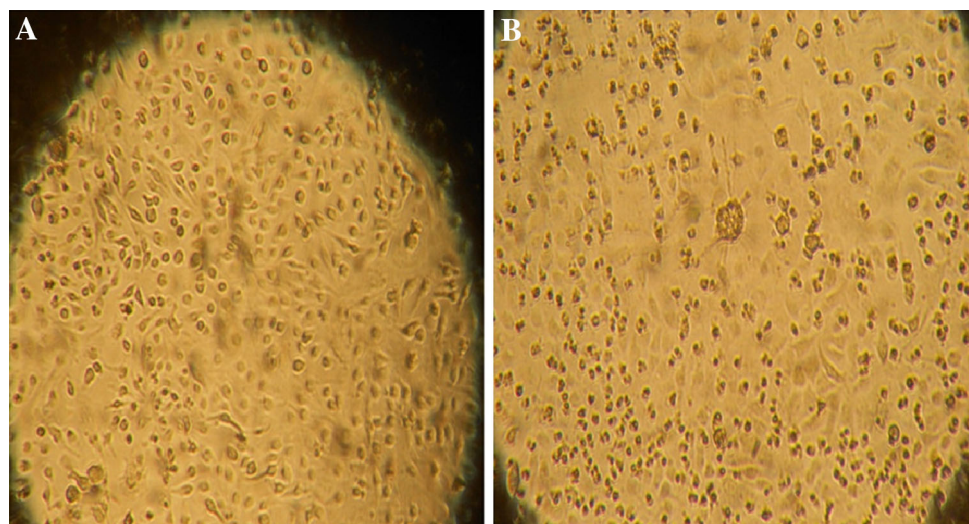
The cancer cells and normal cells grown on glass cover slips were incubated with biosynthesized AgNPs. After the treatment with AgNPs, some morphological alterations were observed during the microscopic examination. The

changes in treated cancer cells were compared with treated normal cells. The morphological changes such as cell shrinkage, retardation of cell growth, cytoplasmic condensation and membrane blebbing were detected in the cancer cells (Fig. 9). The similar results were observed in the earlier report (Kanipandian et al. 2014). However, no such effects were seen in HBL-100 cells, and it was shown with normal morphology (image not given).

#### Conclusion

The biological route of the synthesizing nanoparticles was known to be the eco-friendly, simple and cost-effective. In this study, the silver nanoparticles were successfully synthesized using the plant leaf extract of *Indoneesiella echioides* and were characterized by UV–visible spectroscopy, FTIR, XRD, HR-TEM and SAED pattern. The presence of the spherical silver nanoparticles with average size of  $\sim 29$  nm was synthesized. The present study also confirms the antioxidant activity of biosynthesized silver nanoparticles, which can be effectively used as the drug to eradicate the free radicals to prevent the cellular injury. Due to their high antimicrobial activity, the silver nanoparticles can also be used in the antimicrobial applications. The present study also dealt with the anticancer potential of AgNPs against human lung adenocarcinoma cancer cell line (A549) and normal human epithelial cells (HBL-100), and further study on silver nanoparticles will be carried out for drug delivery, food and pharmaceutical applications.

**Fig. 9** Morphological alterations of AgNPs control (a) and treated (b) A549 lung cancer cells visualized by bright field microscopy



**Acknowledgments** The authors are thankful to the UGC-DAE Consortium for Scientific Research, Indore, for providing financial support through collaborative research project (Ref. No: CSR-I/CRS-71/2015-2016/2101). We are also grateful to UGC-SAP DRS-II for the Instrumentation facilities in the Department of Animal Science, Bharathidasan University, Tiruchirappalli, Tamil Nadu, India.

**Open Access** This article is distributed under the terms of the Creative Commons Attribution 4.0 International License (<http://creativecommons.org/licenses/by/4.0/>), which permits unrestricted use, distribution, and reproduction in any medium, provided you give appropriate credit to the original author(s) and the source, provide a link to the Creative Commons license, and indicate if changes were made.

## References

- Anamika M, Sanjukta C, Prashant MR, Geeta W (2012) Evidence based green synthesis of nanoparticles. *Adv Mater Lett* 3:519–525
- Ankamwar B, Chaudhary M, Sastry M (2005) Gold nanotriangles biologically synthesized using tamarind leaf extract and potential application in vapor sensing. *Synth React Inorg Met* 35:19–26
- Ashok B, Bhagyashree J, Ameeta R, Kumara B, Smita Z (2010) Banana peel extract mediated novel route for the synthesis of silver nanoparticles. *Colloids Surf A Physicochem Eng Asp* 368:58–63
- Dua B, Jiang H (2007) Biosynthesis of gold nanoparticles assisted by *Escherichia coli* DH5a and its application on direct electrochemistry of hemoglobin. *Electrochem Commun* 9:1165–1170
- Dwivedi AD, Gopal K (2010) Biosynthesis of silver and gold nanoparticles using *Chenopodium album* leaf extract. *Colloids Surf A Physicochem Eng Asp* 369:27–33
- Gamble JS (1956) Flora of the presidency of Madras. Botanical survey of India, Calcutta
- Halliwell B, Gutteridge JMC (1999) Free radicals in biology and medicine. Oxford University Press, Oxford
- Huang J, Li Q, Sun D, Lu Y, Su Y, Yang X, Wang H, Wang Y, Shao W, He N, Hong J, Chen C (2007) Biosynthesis of silver and gold nanoparticles by novel sundried *Cinnamomum camphora* leaf. *Nanotechnology* 18:105104–105111
- Huh AJ, Kwon YJ (2011) Nanoantibiotics: a new paradigm for treating infectious diseases using nanomaterials in the antibiotics resistant era. *J Control Release* 156(2):128–145
- Jose Ruben M, Jose Luis E, Alejandra C, Katherine H, Juan BK, Jose Tapia R, Miguel Jose Y (2005) The bactericidal effect of silver nanoparticles. *J Nanotechnol* 16:2346–2353
- Kanipandian N, Thirumurugan R (2014) A feasible approach to phyto-mediated synthesis of silver nanoparticles using industrial crop *Gossypium hirsutum* (cotton) extract as stabilizing agent and assessment of its in vitro biomedical potential. *Ind Crops Prod* 55:1–10
- Kanipandian N, Kannan S, Ramesh R, Subramanian P, Thirumurugan R (2014) Characterization, antioxidant and cytotoxicity evaluation of green synthesized silver nanoparticles using *Cleistanthus collinus* extract as surface modifier. *Mater Res Bull* 49:494–502
- Kannan P, Abraham John S (2008) Synthesis of mercaptothiadiazole functionalized gold nanoparticles and their self-assembly on Au substrates. *Nanotechnology* 19(8):085602
- Kathiraven T, Sundaramanickam A, Shanmugam N, Balasubramanian T (2015) Green synthesis of silver nanoparticles using marine algae *Caulerpa racemosa* and their antibacterial activity against some human pathogens. *Appl Nanosci* 5:499–504
- Kaviya S, Santhanalakshmi J, Viswanathan B, Muthumary J, Srinivasan K (2011) Biosynthesis of silver nanoparticles using *Citrus sinensis* peel extract and its antibacterial activity. *Spectrochim Acta A* 79:594–598
- Kirtikar KR, Basu BD (1975) In Indian medicinal plants-3. Periodical Experts, New Delhi
- Li S, Shen Y, Xie A, Yu X, Zhang X, Yang L, Li C (2007) Rapid, room-temperature synthesis of amorphous selenium/protein composites using *Capsicum annum* L. extract. *Nanotechnology* 18:405101
- Maliszewska I, Sadowski Z, Waszak K (2009) Biological synthesis of silver nanoparticles. *J Phys Conf Ser* 146:012–024
- Moskovitz J, Yim MB, Chock PB (2002) Free radicals and disease. *Arch Biochem Biophys* 397:354–359
- Nadkarni AK, Nadkarni KM (1976) Indian materia medica, vol 1. Popular Prakashan, Bombay
- Qadrie ZL, Jacob B, Anandan R, Raj Kapoor B, Rahamathulla M (2009) Antibacterial activity of ethanol extract of *Indoneesiella echinoides*. *Pak J Pharm Sci* 22:123–125
- Rai M, Yadav A, Gade A (2009) Silver nanoparticles as a new generation of antibacterials. *Biotechnol Adv* 27:76–83
- Rajkumar KS, Kanipandian N, Thirumurugan R (2015) Toxicity assessment on haematology, biochemical and histopathological alterations of silver nanoparticles-exposed freshwater fish *Labeo rohita*. *Appl Nanosci*. doi:10.1007/s13204-015-0417-7
- Rameshkumar A, Sivasudha T (2012) In vitro antioxidant and antimicrobial activity of aqueous and methanolic extract of *Mollugo nudicaulis* Lam. Leaves. *Asian Pac J Trop Biomed* 2(2):S895–S900
- Rao CNR, Cheetham AK (2001) Science and technology of nanomaterials: current status and future prospects. *J Mater Chem* 11:2887–2894
- Savithamma N, Rao ML, Devi PS (2011) Evaluation of antibacterial efficacy of biologically synthesized silver nanoparticles using stem barks of *Boswellia ovalifoliolata* Bal. and Henry and *Shorea tumbugaia* Roxb. *J Biol Sci* 11:39–45
- Sharma VK, Yngard RA, Lin Y (2009) Silver nanoparticles: green synthesis and their antimicrobial activities. *Adv Colloids Interf Sci* 145:83–96
- Sharvil SP, Ravindra SD, Mithun VV, Paradkar AR, Khanna PK (2009) Synthesis and antibacterial studies of chloramphenicol loaded nano-silver against *Salmonella typhi*. *Metal Org Nano-metal Chem* 39:65–72
- Shashi Prabha D, Manu L, Mika S (2010) Green synthesis and characterizations of silver and gold nanoparticles using leaf extract of *Rosa rugosa*. *Colloids Surf A Physicochem Eng Asp* 364:34–41
- Singaravelu G, Arockiamary JS, Ganesh Kumar V, Govindaraju K (2007) A novel extracellular synthesis of monodisperse gold nanoparticles using marine algae, *Sargassum wightii* Greville. *Colloids Surf B Biointer* 57:97–101
- Solomon T, Schimanski A, Sturm H, Illenberger E (2004) Reactions of amide group with fluorine as revealed with surface analytics. *Chem Phys Lett* 387:312–316
- Swamy MK, Sudipta KM, Jayanta K, Balasubramanya S (2014) The green synthesis, characterization, and evaluation of the biological activities of silver nanoparticles synthesized from *Leptadenia reticulata* leaf extract. *Appl Nanosci*. doi:10.1007/s13204-014-0293-6
- Vasanth K, Ilango K, Mohankumar R, Agrawal A, Dubey GP (2014) Anticancer activity of Moringa oleifera mediated silver nanoparticles on human cervical carcinoma cells by apoptosis induction. *Colloids Surf B* 1:354–359
- Vendemiale G, Grattagliano I, Altomare E (1999) An update on the role of free radicals and antioxidant defense in human disease. *Int J Clin Lab Res* 29:49–55

- Weir E, Lawlor A, Whelan A, Regan F (2008) The use of nanoparticles in anti-microbial materials and their characterization. *Analyst* 133:835–845
- Yugandhar P, Savithamma N (2015) Biosynthesis, characterization and antimicrobial studies of green synthesized silver nanoparticles from fruit extract of *Syzygium alternifolium* (Wt.) Walp. an endemic, endangered medicinal tree taxon. *Appl Nanosci*. doi:[10.1007/s13204-015-0428-4](https://doi.org/10.1007/s13204-015-0428-4)
- Zhu M (2000) Apparatus analyses. Higher Education Press, Beijing